Robustness of the remanent magnetic domain pattern formation and associated stripe-bubble transitions in Co/Pt multilayers against field sequencing

Aaron Gentillon, Carson Richards, Luis A. Ortiz-Flores, Jeremy Metzner, David Montealegre, Matthew Healey, Kelsey Cardon, Andrew Westover, Olav Hellwig, and Karine Chesnel

COLLECTIONS

Paper published as part of the special topic on 65th Annual Conference on Magnetism and Magnetic MaterialsMMM2021

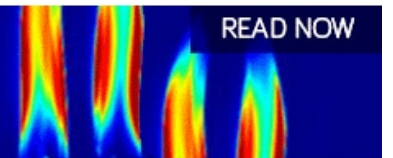# Robustness of the remanent magnetic domain pattern formation and associated stripe-bubble transitions in Co/Pt multilayers against field sequencing

View Online   Export Citation   CrossMark

Aaron Gentillon,[1] [iD] Carson Richards,[1] Luis A. Ortiz-Flores,[1,2] Jeremy Metzner,[1] David Montealegre,[1] Matthew Healey,[1] Kelsey Cardon,[1] Andrew Westover,[1] Olav Hellwig,[3,4] [iD] and Karine Chesnel[1,a]

AFFILIATIONS

[1] Department of Physics and Astronomy, Brigham Young University, Provo, Utah 84602, USA
[2] Department of Physics Applied to Electronics, Universidad de Puerto Rico-Humacao, Humacao, Puerto Rico 00792, USA
[3] Institute of Ion Beam Physics and Materials Research, Helmholtz-Zentrum Dresden-Rossendorf, Bautzner Landstrasse 400, 01328 Dresden, Germany
[4] Institute of Physics, Chemnitz University of Technology, 09107 Chemnitz, Germany

Note: This paper was presented at the 65th Annual Conference on Magnetism and Magnetic Materials.
[a] Author to whom correspondence should be addressed: kchesnel@byu.edu

ABSTRACT

Thin ferromagnetic [Co/Pt] multilayers with perpendicular magnetic anisotropy exhibit a variety of nanoscopic magnetic domain patterns at remanence, from long interlaced stripes to lattices of bubbles, depending on the multilayer structure but also on the magnetic history of the sample. For optimized structural parameters, stripe-bubble transitions accompanied by drastic increases in domain density have been observed when the magnitude of the previously applied perpendicular field H_m is finely tuned throughout the hysteresis loop. Here, we investigate the robustness of these morphological transitions against field sequencing and field cycling. We conducted this study on $[Co(x)/Pt(7Å)]_{N=50}$ where x varies from 4 to 60 Å. We mapped the morphological transition with H_m varying from 0 to 9 T, following both an ascending sequence ($0 \rightarrow 9$ T) and a descending sequence (9 T $\rightarrow 0$). We found that the optimal field $H_m = H^*$ at which the domain density is maximized and its associated maximal density n^* are not significantly affected by the field sequencing direction. We have also investigated possible pumping effects when cycling the applied field at the value H^*. We found that n^* remains relatively stable through field cycling, and much more stable in the bubble state, compared to longer stripe states. The observed robustness of these morphological transitions against field sequencing and field cycling is of crucial importance for potential magnetic recording applications.

I. INTRODUCTION

Due to their nanometric size and their variety of morphologies, magnetic domains in thin ferromagnetic films with perpendicular magnetic anisotropy (PMA) provide many interesting features for technological applications, such as magnetic recording nanotechnologies,[1,2] but also for studying complex physical phenomena, including interlayer magnetic domain couplings,[3] magnetic domain memory,[4–7] and the formation of magnetic textures such as lattices of magnetic vortices[8] and skyrmions.[9] Some of the motivations driving the development of new magnetic textures for nanotechnological applications include the reduction of domain sizes down to below ~ 50 nm and the associated maximization of domain densities. In this paper, we focus on morphological stripe-bubble transitions occurring in thin PMA ferromagnetic films, where the domain density at remanence is drastically enhanced by a factor of 10 or more, from a hundred to thousands of individual disconnected domains per 100 μm^2 area.[10] Due to the high density, these domains then transform from elongated stripes to circular bubbles. We observed these morphological transitions in the remanent domain patterns exhibited by $[Co/Pt]_N$ multilayered thin films, where the thicknesses

of the Co and Pt layers and the number of repetitions N are optimized for producing nanometric magnetic domains with perpendicular magnetization.[11,12] In these systems, we are able to induce and control the morphological stripe-bubble transitions in the remanent domain patterns by finely tuning the magnitude H_m of the previously applied out-of-plane (OOP) external magnetic field.

In our previous studies of the magnetic stripe –bubble transitions in Co/Pt multilayers[10,11] we have shown the existence of an optimal value H^* for H_m at which the density n of the reverse domains (for which the magnetization is opposite to the direction of the previously applied OOP field) in the remanent pattern is significantly increased, while keeping the net magnetization of the material close to zero (no remanence). When H_m is finely tuned to H^*, the remanent domain pattern, which initially forms a maze of long interlaced stripes, gradually transforms into a set of short bubble-like domains and even into lattices of small closely packed bubbles for specific [Co/Pt] structural parameters.[12] Our purpose in this paper is to investigate the robustness of the occurrence of these morphological magnetic transitions throughout field sequencing and field cycling, in particular the reliability of H^* and the stability of the associated maximal density n^* as the magnetic field is cycled.

II. MATERIAL AND PREVIOUS RESULTS

In this paper, we focus on a series of $[Co(x)/Pt(7\ \text{Å})]_{N=50}$ multilayers where the Co thickness x is set to a value between 4 and 60 Å The series includes eight samples, for which x = 4, 8, 12, 16, 25, 31, 40 and 60 Å, respectively. For each Co thickness, the Co/Pt bilayer is repeated N = 50 times. As illustrated by the sketch in Fig. 1a,

these multilayers were deposited on silicon wafers covered with a native silicon oxide layer, a 15 Å tantalum seeding layer and a 200 Å platinum buffer layer. The multilayers are covered by a protective capping layer of 23 Å of platinum. In our previous studies,[11,12] we investigated the structural and magnetic properties of these multilayers and found that all the multilayers of various Co thicknesses with N = 50 are highly crystalline, present an effective perpendicular magneto-crystalline anisotropy and exhibit OOP magnetic domain patterns.

A comparative display of the major OOP magnetization loops for the eight samples shown in Fig. 1b indicates that the saturation field H_s gradually increases with the Co thickness t_{Co}. The magnetization loops all show a similar shape, with nearly zero remanence (M = 0 at H = 0), a reversible portion centered around the origin, and some hysteresis occurring at higher field near saturation H_s.

In our previous studies[10,11] we have established the occurrence of morphological transitions in the domain pattern at remanence when a series of minor OOP loops are applied and the magnitude H_m of the previously applied field is finely tuned between zero and H_s. We found that for all the Co thicknesses, there exists an optimal value H^* for H_m at which the domain density n at remanence is maximized. The value H^* lies around 80-90 % of H_s depending on the Co thickness. The observed magnetic domain pattern at remanence typically evolves from a long-stripe mazy state when $H_m < H^*$ to a short-stripe state or bubble state when $H_m \approx H^*$ and an intermediate stripe state when $H_m > H^*$. This morphological transition is illustrated in Fig. 1c for t_{Co} = 25 Å (not featured in previous publications) for which H^* = 9.3 kOe. Fig. 1c features the reverse density plot $n(H_m)$ along with a selection of magnetic domain patterns collected
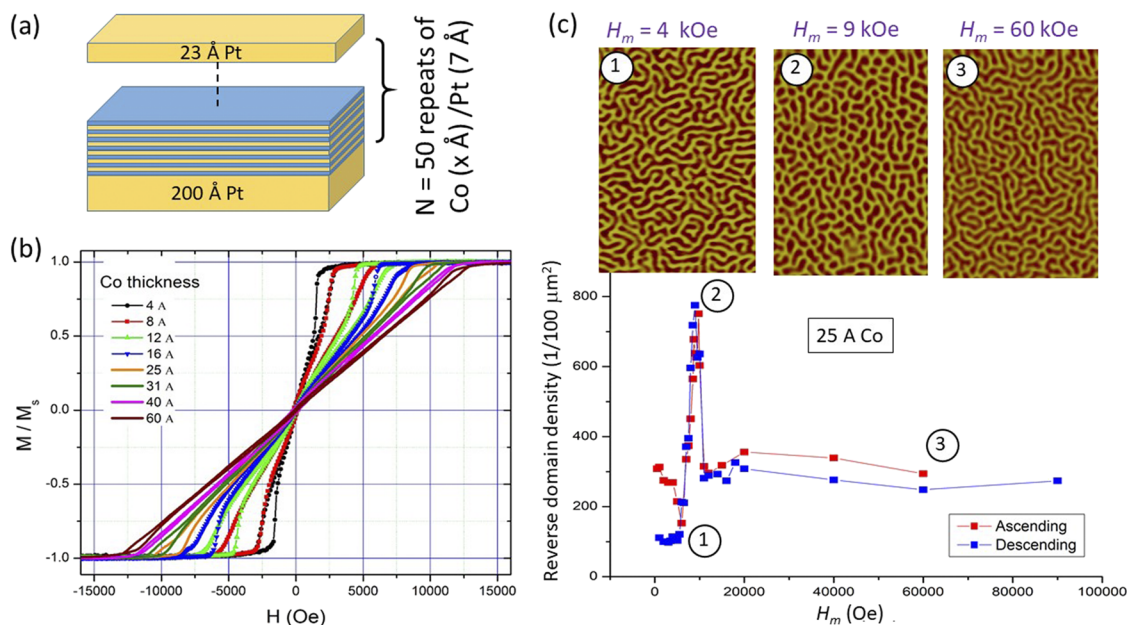
FIG. 1. Overview of the magnetic behavior of the material. (a) Sketch of the $[Co(x)/Pt(7\ \text{Å})]_{N=50}$ multilayers studied in this paper; (b) Set of magnetization loops measured with magnetic field applied out-of-plane for various Co thicknesses t_{Co}, varying from 4 to 60 Å; (c) Domain density plots $n(H_m)$ measured for t_{Co} = 25 Å following the ascending and descending sequences. Also pictured is a selection of magnetic domain patterns (imaged via MFM) collected at the various magnitudes H_m indicated on the density plot.

via magnetic force microscopy (MFM) at specific value H_m indicated on the $n(H_m)$ curve. When H_m = 4 kOe < H^*, the domains are long, form a maze, and the density is as low as 100 domains/100 μm^2, whereas when H_m = 9 kOe ~ H^*, the domains are very short, some of them being in a bubble form, and the density peaks, approaching 800 domains/100 μm^2. When H_m = 60 kOe > H^*, the domains are elongated again, reaching an intermediate size and the domain density plateaus at around 300 domains/100 μm^2.

In the present study, we investigate the robustness of the observed morphological transition in the magnetic domain pattern at remanence against the sequencing order of the previously applied OOP magnetic field H_m. We also want to see if repeatedly cycling the field at H_m = H^* would potentially lead to "pumping" effects, causing a further increase in domain density.

III. METHODS

To study the effect of field sequencing and field cycling on the morphological magnetic transitions in the [Co/Pt] multilayers, various sequences of magnetic field cycles were applied in the OOP direction and magnetic domain patterns were collected at remanence between each cycle. A field cycle consists in applying an OOP magnetic field of magnitude H_m following a (0 → - H_m → + H_m → 0) loop. Three types of sequencing series were applied as follows:

(1) **Ascending series:** the magnitude H_m of the loop is gradually increased from 0 to 9 T.
(2) **Descending series:** the magnitude H_m of the loop is gradually decreased from 9 T to zero.

(3) **Pumping series:** the applied field is being cycled multiple times at the same value H_m = H^* where the domain density was observed to be maximized.

For each of the eight $[Co(x)/Pt(7\text{Å})]_{N=50}$ samples, where x varies from 4 to 60 Å, several ascending and descending series were measured and compared. A pumping series was applied to the t_{Co} = 8 Å sample at H^* = 0.52 T, as well as the t_{Co} = 31 Å sample at H^* = 0.97 T. Domain densities were plotted as a function of number of field cycles, or "pumps."

The magnetization loops were applied via Vibrating Sample Magnetometry (VSM) using a Quantum Design Physical Properties instrument, including a 9 T superconducting magnet. For this entire study, the magnetic field was applied in the OOP direction, i.e., perpendicular to the multilayers plane. The magnetic domain patterns were imaged via MFM using a Dimension 3100 Veeco Digital Instruments by Bruker and magnetically coated etched silicon probe (MESP) tips. Typical image sizes were 10 x 10 μm^2. The MFM images were analyzed computationally via a flood fill algorithm in order to extract the density of the domains with magnetization direction respectively aligned with, and opposite to the direction of the previously applied field. These domain densities, typically expressed per unit of 100 μm^2, are then plotted as a function of magnitude H_m and Co thickness t_{Co}. The resulting density maps allow to visualize the morphological transition between the maze pattern, short stripe patterns and bubble patterns. Various cuts through the maps were applied and compared to explore the effect of field sequencing on these morphological transitions.
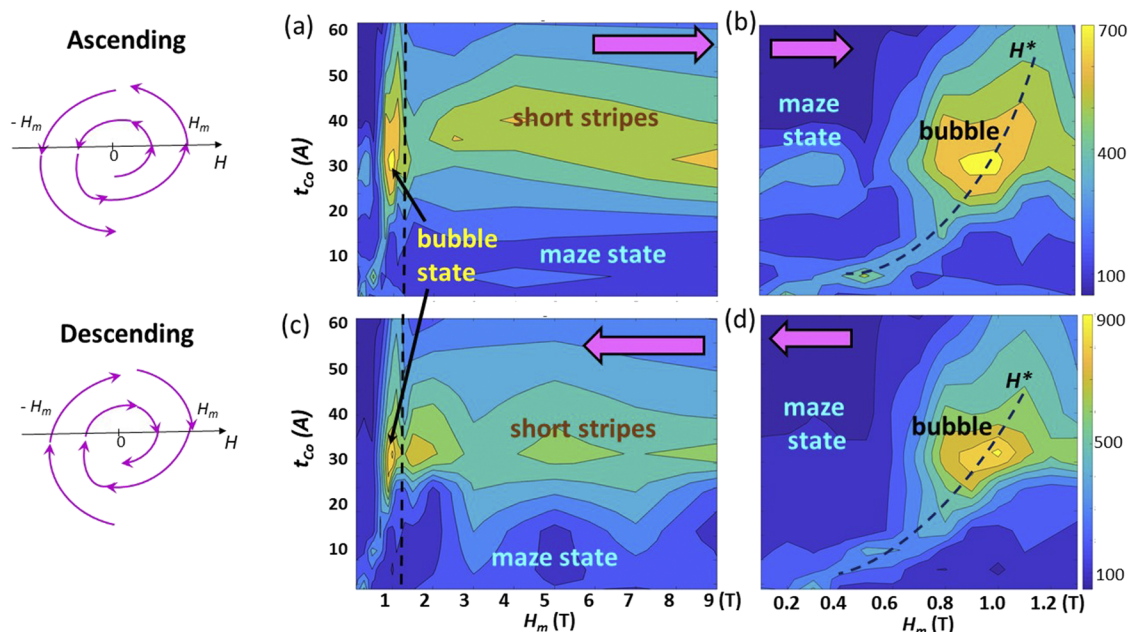
FIG. 2. Density maps $n(t_{Co}, H_m)$ plotting the density of the reverse domains at remanence as a function of previously applied field H_m for the various Co thicknesses t_{Co}, measured following the ascending sequence (a) with enlargement (b) and the descending sequence (c) with enlargement (d). Panels (a) and (c) show the density maps on the full [0-9T] range for H_m. Panels (b) and (d) show an enlarged view of the [0.1-1.3 T] range for H_m.

IV. RESULTS AND DISCUSSION

Here, we review the results obtained for two types of studies: comparing ascending and descending sequences, on one hand, and studying the response to field cycling at H^*, on the other hand.

### A. Ascending versus descending sequencing comparison

Multiple ascending and descending series were collected for each of the eight Co thicknesses. The resulting average density maps $n(t_{Co}, H_m)$ for the ascending and the descending sequences are displayed in Fig. 2. In these maps, the density n of the reverse domains (with magnetization opposite to the previously applied field) in the remanent domain pattern is plotted and interpolated as a function of Co thickness t_{Co} and of H_m, over a wide [0 – 9 T] range. The ascending map in Fig. 2a with enlargement in Fig. 2b and the descending map in Fig. 2c with enlargement in Fig. 2d show similar features: a

narrow, sharp density peak and a ridge situated at $t_{Co} \approx 30$ Å. Closer views on the peak region, using a [0 – 1.2 T] range for H_m, displayed in Fig. 2b for the ascending sequence and Fig. 2d for the descending sequence show a similar behavior for the ascending and descending series, with a density peak of about the same shape and size, situated at the same location on the maps.

To compare the ascending and descending behaviors quantitatively, we have plotted and fitted a selection of density curves $n(H_m)$ measured at fixed Co thickness. A first example of comparison was shown in Fig. 1c for $t_{Co} = 25$ Å. At first sight, the shape of the $n(H_m)$ curves for the descending and ascending sequences is very similar, with a peak located at the same position H^* and of about the same height n^*. A close-up view on the peak in the $n(H_m)$ curves for each of the eight Co thicknesses is shown in Fig. 3(a-h). The measured data points are plotted along with fitting curves for both the ascending and descending series for direct comparison. These comparative plots indicate a general agreement between the ascending
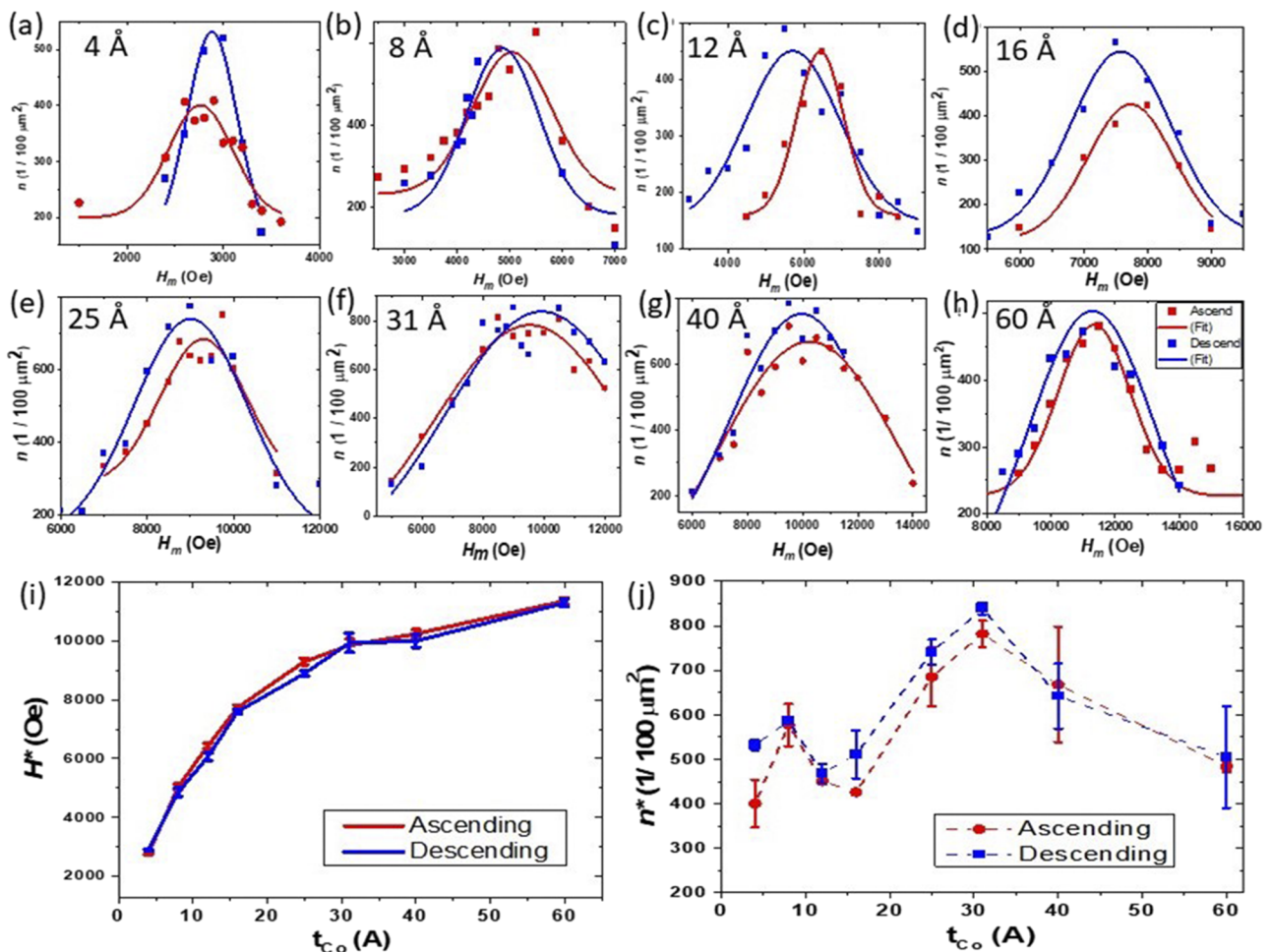
FIG. 3. Comparative analysis of the remanent domain density, for the ascending sequence (red circles) and the descending sequence (blue squares). (a)–(h) Density plots $n(H_m)$ around their peak position H^* for the various t_{Co} (indicated on the graphs), including data points along with fits. (i) Fitted value for H^* as a function of t_{Co}. (j) Fitted value for n* as a function of t_{Co}. For both the H^* and n^* graphs, the displayed value is an average over multiple measurements and the error is calculated using the experimental standard deviation.
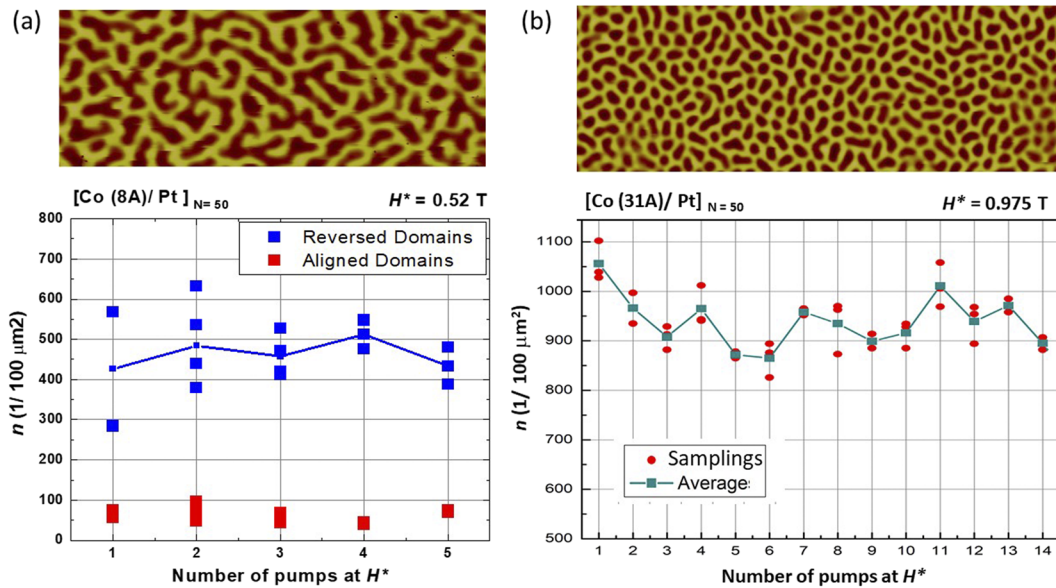
FIG. 4. Field cycling studies, displaying the remanent domain density n as a function of field cycle at $H_m = H^*$ along with MFM images of the magnetic domain patterns: (a) for $t_{Co} = 8$ Å, for which $H^* = 0.52$ T and where the domain pattern consists of short-medium stripes (b) for $t_{Co} = 31$ Å, for which $H^* = 0.975$ T and where the domain pattern consists of mostly bubbles.

and descending sequences, with some slight random and not systematic discrepancies in peak position H^* and peak width, and some more systematic differences in peak height n^* (with the descending sequence always showing a higher or equal density compared to the ascending sequence).

The fitted H^* value averaged over multiple measurements for both the ascending and descending sequences displayed in Fig. 3i shows an excellent agreement. For both sequencing orders, the fitted value H^* consistently increases with t_{Co}. The discrepancy ΔH^* between the ascending and descending sequences is generally less than 5% with standard deviations on the fitted H^* values being on the order of 2-3%. The associated fitted density n^* curves displayed in Fig. 3j for both the ascending and the descending sequences indicates a consistent trend, exhibiting a peak at $t_{Co} \approx 30$ Å The discrepancy Δn^* between the ascending and descending sequences varies from as low as 2% to as high as 25%, but is mostly in the 5-15% range. Observed variations between multiple measurements in the same sequencing order indicate that the experimental uncertainty on n^* (plotted as error bars for both the ascending and the descending curves) may also reach up to 25 % and be mostly responsible for the observed discrepancy between the ascending and descending curves.

B. Response to field cycling at H^*

The observation of a sharp peak located at t_{Co} ~30 Å in the domain density maps triggers the question of the possibility of "pumping" or increasing the density further by field cycling. We investigate the response of the material when cycling the field at $H_m = H^*$ for two different Co thicknesses for comparison purposes: the optimal thickness $t_{Co} = 31$ Å and the lower thickness $t_{Co} = 8$ Å. The

results are displayed in Fig. 4. In the case of $t_{Co} = 8$ Å, for which $H^* \approx 0.5$ T, the domain pattern after field cycling at H^* is made of medium size interlaced stripes and the associated domain density approaches 500 domains/100 μm^2. The plot in Fig. 4a indicates that after five cycles, despite some relatively large variations, the density (averaged over multiple MFM images at each cycle) remains statistically at about the same level, averaging about 465 ± 100 domains/100 μm^2.

For $t_{Co} = 31$ Å, on the other hand, the domain pattern exhibited at $H^* \approx 0.97$ T is made of very small, bubble-like domains that are closely packed and for which n may exceed 1000 domains/100 μm^2. The graph in Fig. 4b, which plots the measured domain densities estimated from various MFM samplings throughout multiple successive field cycles, suggests that cycling the field does not cause any pumping effect or increase in n. However, the data shows that even after 14 cycles at H^*, n remains relatively stable, averaging about 945 ± 35 domains/100 μm^2. In other words, the variations in n over that many cycles are on average less than 4 %. These variations for $t_{Co} = 31$ Å are remarkably small compared to the $t_{Co} = 8$ Å case, for which density variations can reach up to about 20%. Part of this discrepancy may be due to the lower domain density, about half, and consequently higher relative statistical Poisson noise in the $t_{Co} = 8$ Å case, compared to the $t_{Co} = 31$ Å case. While the Poisson noise for a density of 1000 domains/100 μm^2 is about 3.7% and fully explains the density variations for the $t_{Co} = 31$ Å sample, the Poisson noise calculated on a density of 500 domains/100 μm^2 is about 5% only, and does not explain the observed density variations for the $t_{Co} = 8$ Å sample. This suggests that domain densities are more reliable and reproducible when the domain pattern is in a short stripe state or bubble state compared to elongated stripe states.

V. CONCLUSION

We have investigated the morphological stripe-bubble transitions in remanent magnetic domain patterns in $[\text{Co}(x)/\text{Pt}(7 \text{ Å})]_{N=50}$ multilayers with $4 \leq x \leq 60$ Å and their robustness throughout field cycling while applying an OOP magnetic field. By mapping the domain density n versus the field magnitude H_m for various Co thicknesses x, we found that these transitions are robust with respect to field sequencing. In particular, the optimal field $H_m = H^*$ at which n is maximized remains unchanged when applying ascending and descending field sequences, with less than 5% variations. When successively cycling the field at the value $H_m = H^*$, the associated maximal domain density n^* remains relatively stable. The data suggests that the smaller the domain size, the higher the stability of n^*. When the domain pattern is made of short stripes, as observed for $x = 8$ Å for which $n^* \sim 500$ domains/100 μm^2, the variations in n^* with field cycling may reach up to $\pm 20\%$, whereas when the domain pattern is made of small bubbles, as observed for $x = 30$ Å for which $n^* \sim 1000$ domains/100 μm^2, n^* remains stable within $\pm 5\%$ upon cycling the field at H^*. The stability in n^* may be further improved when n^* is further increased to beyond 2000 domains/100 μm^2 as it does for the lattices of monodisperse bubbles observed in $[\text{Co}(30\text{Å})/\text{Pt}(7\text{Å})]_{N=20}$ multilayers.[12] The observed robustness of the stripe-bubble transitions against field sequencing and field cycling and relative stability of optimized densities n^* are crucial properties for potential magnetic recording applications.

ACKNOWLEDGMENTS

DATA AVAILABILITY

The data that support the findings of this study are available from the corresponding author upon reasonable request.

REFERENCES

[1] N. S. Kiselev, A. N. Bogdanov, R. Schäfer, and U. K. Rößler, J. Phys. D **44**, 392001 (2011).

[2] A. Fert, N. Reyren, and V. Cros, Nat. Rev. Mater. **2**, 17031 (2017).

[3] O. Hellwig, A. Berger, J. B. Kortright, and E. E. Fullerton, J. Magn. Magn. Mater. **319**, 13 (2007).

[4] K. Chesnel, in *Magnetism and Magnetic Materials*, edited by N. Panwar (InTechOpen, London, UK, 2018), Chap. 3.

[5] M. Pierce, C. R. Buechler, L. B. Sorensen, J. J. Turner, S. D. Kevan, E. A. Jagla, J. M. Deutsch, T. Mai, O. Narayan, J. E. Davies, K. Liu, J. Hunter Dunn, K. M. Chesnel, J. B. Kortright, O. Hellwig, and E. E. Fullerton, Phys. Rev. Lett. **94**, 017202 (2005).

[6] K. Chesnel, E. E. Fullerton, M. J. Carey, J. B. Kortright, and S. D. Kevan, Phys. Rev. B **78**, 132409 (2008).

[7] K. Chesnel, A. Safsten, M. Rytting, and E. E. Fullerton, Nature Commun. **7**, 11648 (2016).

[8] A. Wachowiak, J. Wiebe, M. Bode, O. Pietzsch, M. Morgenstern, and R. Wiesendanger, Science **298**, 577 (2002).

[9] A. Fert, V. Cros, and J. Sampaio, Nature Nanotech. **8**, 152 (2013).

[10] A. S. Westover, K. Chesnel, K. Hatch, P. Salter, and O. Hellwig, J. Magn. Magn. Mater. **399**, 164 (2016).

[11] K. Chesnel, A. S. Westover, C. Richards, B. Newbold, M. Healey, L. Hindman, and T. Schneider, Phys. Rev. B **98**, 224404 (2018).

[12] L. Fallarino, A. Oelschlägel, J. A. Arregi, A. Bashkatov, F. Samad, B. Böhm, K. Chesnel, and O. Hellwig, Phys. Rev. B **99**, 024431 (2019).